SAND84-0020 Distribution
Unlimited Release 94e
Printed March 1984

EXPERIMENTAL STUDIES OF SALT CAVITY LEACHING VIA FRESH-WATER INJECTION

Daniel C. Reda and Anthony J. Russo
Fluid and Thermal Sciences Department
Sandia National Laboratories, Albuquerque, New Mexico 87185

Abstract

Salt cavity leaching experiments were conducted in the laboratory in support of the U. S. Strategic Petroleum Reserve (SPR) program. Cavities of an initial cylindrical geometry were oreated by machining (hollowing-out) salt cores from one end, leaving the circular wall and bottom as an integral piece. In each of three separate experiments, a salt cavity was placed vertically in a pressure vessel and its interior filled with saturated brine. The vessel was sealed and pressurized to actual SPR-cavern pressure. Fresh water was injected down a tube and into the cavity, while brine was simultaneously removed from the cavity through a second (withdrawal) tube. Both "direct" (injection below withdrawal) and "reverse" (injection above withdrawal) leaching procedures were investigated for essentially the same flowrate conditions and total withdrawal time, A traversable gamma-beam densitometer was positioned between the injection and withdrawal locations in each case, and was used as a non-intrusive diagnostic technique to investigate transient phenomena which occurred during the leaching, and post-leaching (return-to-equilibrium) periods. Beam attenuation measurements yielded a quantitative measure of two (combined) effects: (1) the total (time-integrated) salt-wall recession and (2) the instantaneous (path length-averaged) brine salinity. Final cavity shapes were measured both by gamma-beam densitometry and by sectioning/micrometer techniques. Transient and steady-state measurements were then compared with numerical predictions, generated with SANSMIC (the Sandia Solution-Mining Code), in order to assist in the qualification of this code for actual SPR-cavern applications. Experimental results and numerical predictions were found to be in good agreement.

CONTENTS

	Page
Introduction	7
Experimental Approach	10
Experimental Results versus Numerical Predictions	14
Conclusions	29
References	30

FIGURES

		Page
Figure 1.	SPR Cavern Leaching Schematic	9
Figure 2.	Schematic of Experiment	11
Figure 3.	Gamma-Beam Densitometry, A Schematic	12
Figure 4.	Photograph of Gamma-Beam System and Test Vessel	15
Figure 5.	Photograph of Salt Cavity Model	16
Figure 6.	Transient Count-Rate Distribution, LCH1, Data vs. Predictions	19
Figure 7.	Post-Test Cavity Shapes, LCH1, Data vs. Predictions	20
Figure 8.	Transient Count-Rate Distribution, LCH2, Data vs. Predictions	22
Figure 9.	Post-Test Cavity Shapes, LCH2, Data vs. Predictions	23
Figure 10.	Transient Count-Rate Distribution, LCH3, Data vs. Predictions	26
Figure 11.	Post-Test Cavity Shapes, LCH3, Data vs. Predictions	27

TABLES

Table 1.	Summary of Test Conditions	17

NOMENCLATURE

d	beam diameter (cm)
I	unattenuated beam intensity after passage through material(s) (particles/sec)
I_o	unattenuated beam intensity at source exit (particles/sec)
$\overline{Q}$	average volumetric flowrate (cm^3/min)
R	count rate (particles/sec)
r	cavity radius (cm)
SC	brine specific gravity
t	time (min)
X	vertical coordinate, measured from the initial cavity bottom (cm)
z	coordinate measured along beam pathlength (cm)
ε	salt-wall recession (cm)
μ	gamma-beam linear attenuation coefficient (l/cm>
$\overline{\rho}$	average density (g/cm^3)
τ	electronics system time constant (μsec)

<u>Subscripts</u>

B	brine
i	material i
INJ	injection
SB	saturated brine
WD	withdrawal

INTRODUCTION

The United States Strategic Petroleum Reserve consists of an underground oil storage system comprised of caverns which have been leached in salt domes looated in the Gulf Coast states of Louisiana and Texas. Some of the cavern space, formed during commercial brining operations, was available for oil storage shortly after the SPR program began in the mid-1970's. However, since the available volume was less than that required for the storage of 250 million barrels of oil, and a storage of up to one billion barrels was contemplated, the Repartment of Energy (DOE) undertook an extensive new cavern leaching program.

Since the end of 1978, Sandia National Laboratories has been serving as a technical consultant to the DOE on various aspects of the SPR program, including the cavern leaching and filling efforts. Early experimental and theoretical work on salt dissolution rates and salt cavity formation techniques[1-7] led to the development of three numerical models to predict solution mining processes[7-9]. Of these three, the computer code of Saberian[7] was utilized early in the SPR program to help define initial cavern leaching schedules.

Because there was an urgency to form and fill the reserve as rapidly as possible, considerable attention was given to devising a leaching scheme which would yield not only the desired size and shape of cavern, but would do it in the shortest practical time. This appeared to be best accomplished by using a "leach-fill" strategy in which the cavern would be simultaneously filled with oil as the leaching proceeded. To start the cavern, several wells could be drilled and simultaneously leached until the cavities coalesced to form the final storage volume. The majority of the final volume would ultimately be filled with crude oil, overlying a small saturated-brine pocket located at the cavern bottom, Oil withdrawal from such caverns would then be accomplished by injecting fresh water down a pipe to a level below the "initial" saturated-brine/oil interface, buoyantly displacing the oil upwards,where it would then be removed through a production pipe whose entrance was located near the top of the cavern.

Considering these leaching, filling, and withdrawal processes, it became apparent that there was a need to numerically model "moving interface problems" (i.e., salt dissolution below an oil interface whose location varies with time). Since the Saberian code[7] was not structured to treat such problems in an efficient manner, and since it would be necessary to perform a very large number of computer simulations of these various processes, a new code was developed[10,11]. This code, called SANSMIC (the Sandia Solution-Mining Code), utilizes the same dissolution model as the Saberian code[7], but it includes new diffusion, plume[12,13], and insolubles models, It also incorporates an implicit numerical formulation which significantly reduces computer run times. Cavern geometries are treated as two-dimensional/axisymmetric.

Experiments were conducted[14] to answer one of the basic questions concerning the proposed oil-withdrawal procedure: would crude oil adherence/penetration protect the salt from dissolution following passage of the upward-moving oil/brine interface? Results showed that such "protection" would not occur, and that the proposed oil-withdrawal procedure should not adversely affect cavern shape change in actual field applications.

In a follow-up investigation, reported here, salt cavity leaching (i.e., shape change in the absence of any crude oil) was investigated. This "cavern-formation" problem is summarized by the schematic of Fig, 1.

Objectives of the present research were to experimentally investigate transient salt/brine interactions inside a pressurized salt cavity subjected to leaching via fresh-water injection, and to measure resultant cavity shape change for use in model-validation efforts. The primary independent variable in these studies was the relative vertical position of the injection and withdrawal lines. Both "direct" (injection below withdrawal) and "reverse" (injection above withdrawal) leaching procedures were investigated.

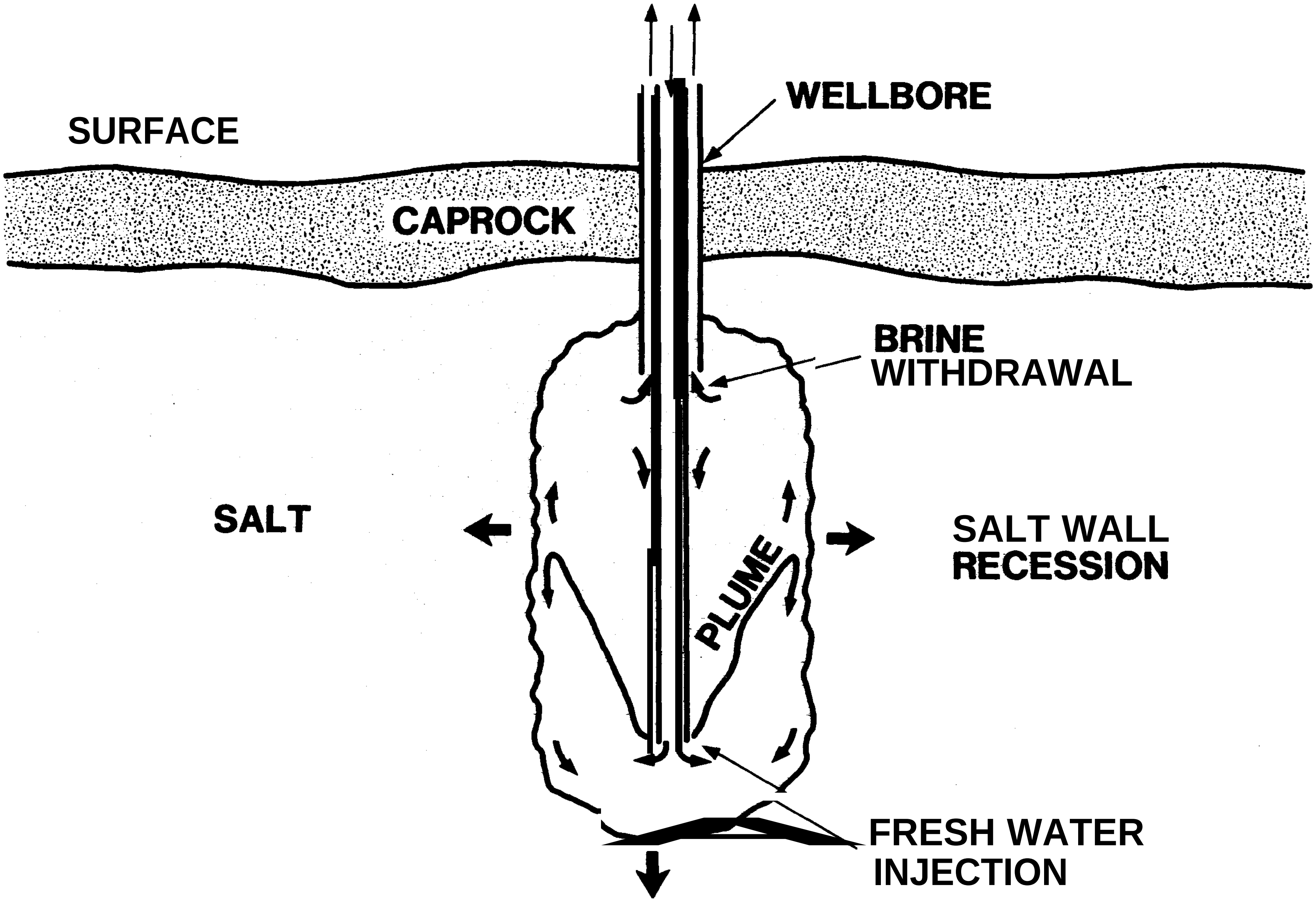

Fig. 1: SPR Cavern Leaching Schematic

EXPERIMENTAL APPROACH

The experimental approach, apparatus, and instrumentation system applied to the salt cavity leaching problem were identical to those utilized (and described) in the oil-withdrawal study[14], and consequently, will not be discussed in any detail here. Figure 2 shows a schematic of the apparatus. Figure 3 summarizes the instrumentation system and its defining equations[15].

The measurement capabilities of the single-energy/single-beam system used in this study are summarized as follows (refer to Fig. 3). The measured count rate, R, is proportional to the number of photons which traverse the experiment and remain in an unattenuated state. Knowing $\tau(R)$ from previous calibrations[14] allows R to be converted to intensity I. For a known I_o, the exponential attenuation law then allows the determination of any <u>one</u> unknown quantity, either an attenuation coefficient (μ_i) or a pathlength of material (z_i).

In the present experiment, all initial pathlengths and material attenuation coefficients were measured prior to the start of leaching. It was found, however, that the attenuation coefficient for brine was a linear function of the mass-fraction of solid salt dissolved in it[14]. Thus, during leaching, <u>two</u> unknowns existed at any vertical position inside the cavity: $\varepsilon(t)$, the total salt-wall recession which occurred up to time t, and $SG(t)$, the instantaneous specific gravity of the brine (pathlength averaged across the cavity interior). Independent measurements of $SG(X,t)$ were not attempted in the present research. Consequently, the observed $R(t)$ response provided a quantitative measurement of the <u>combined</u> effects of total salt-wall recession and instantaneous brine salinity. Such measurements were made both during the leaching process and during the post-leaching (return-to-equilibrium) period.

Upon the re-attainment of an equilibrium state (saturated brine) everywhere within the cavity, the gamma-beam system was traversed vertically along the cavity centerline to measure $\varepsilon(X)$, the only unknown under such conditions. Post-test sectioning of each cavity specimen provided a second measurement of the final cavity shape.

SCHEMATIC OF EXPERIMENT

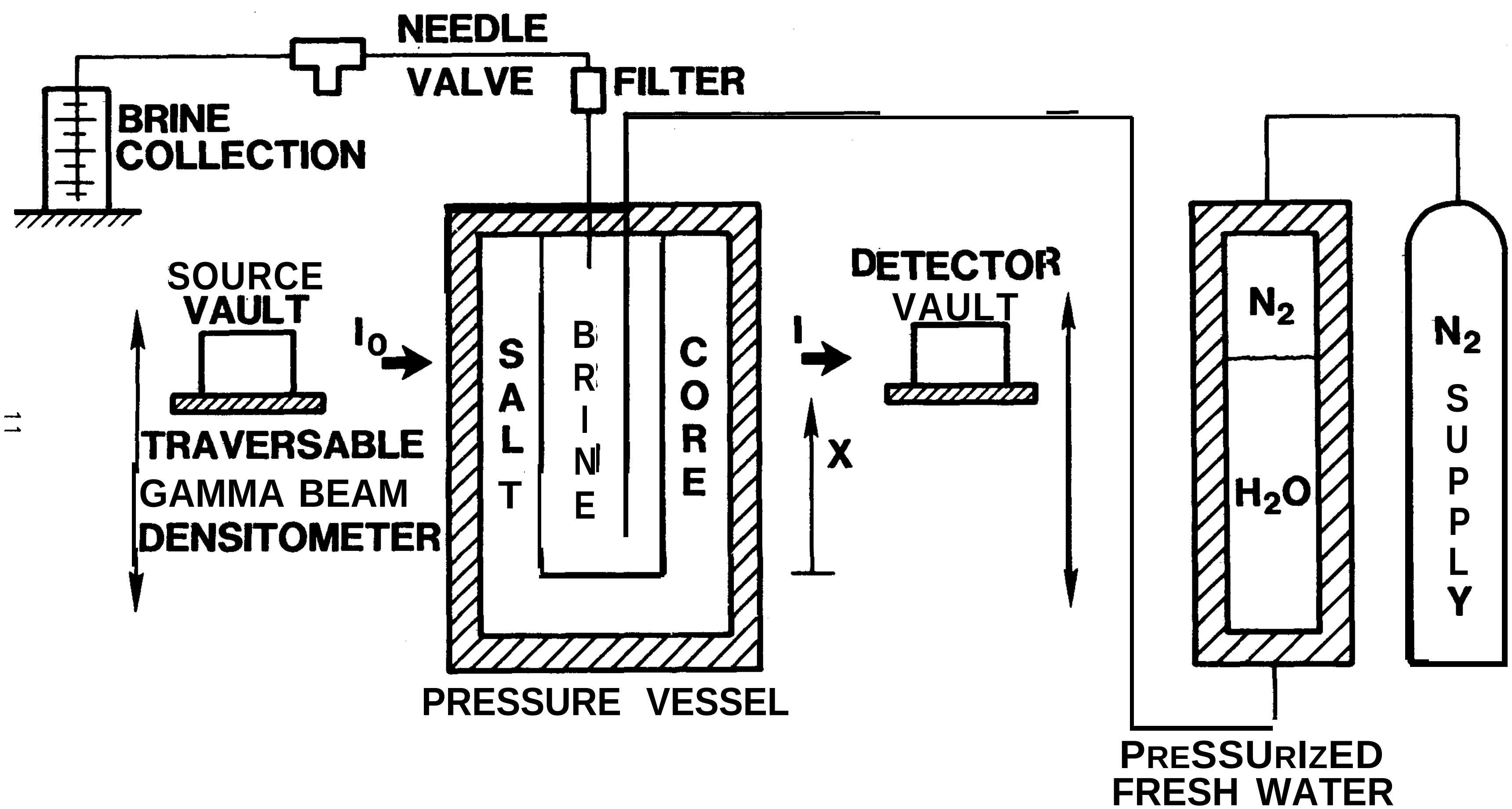

Fig. 2: Schematic of Experiment

GAMMA-BEAM **DENSITOMETRY,** A SCHEMATIC

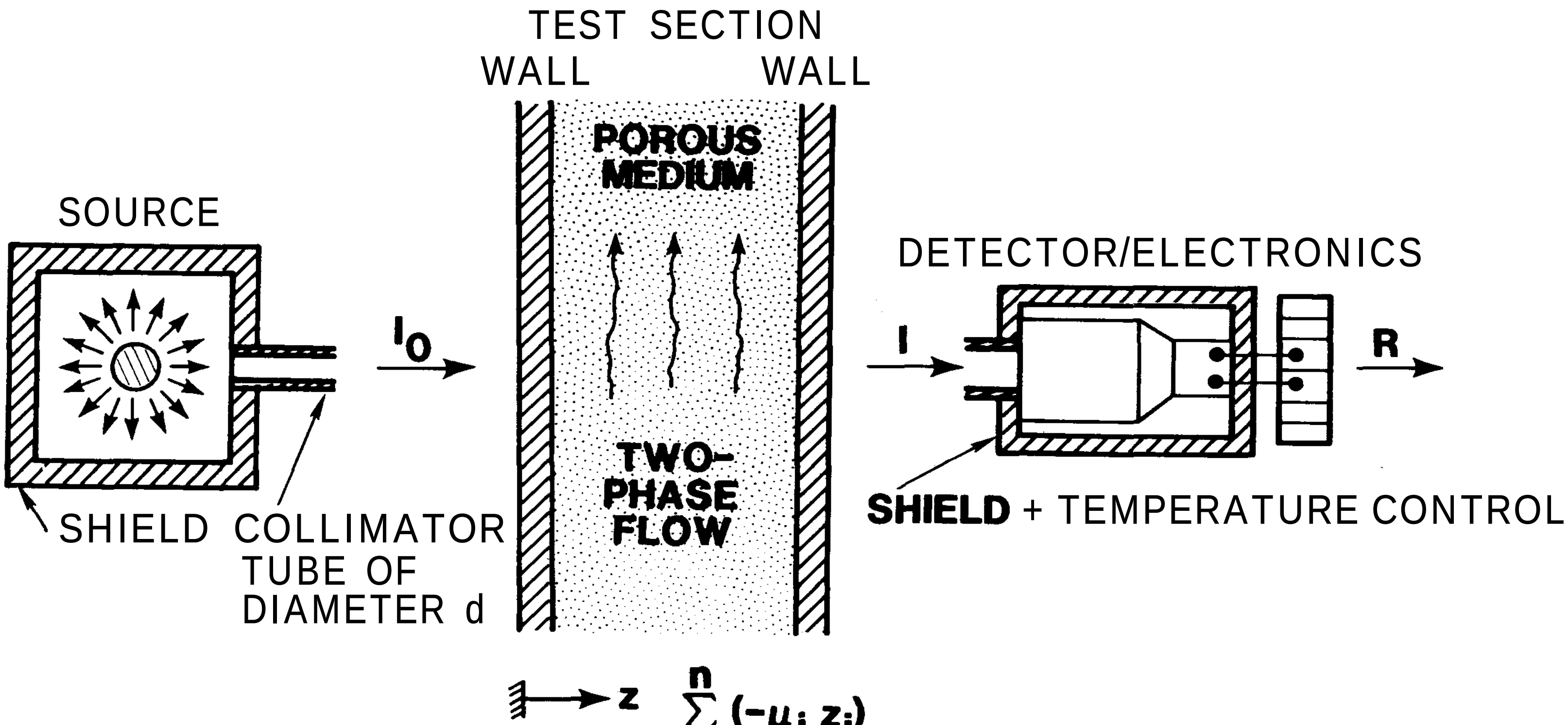

$$I_0 = I_0 (d^2)$$

$$I = I_0 e^{\sum_{i=1}^{n} (-\mu_i z_i)}$$

$$R = \frac{I}{(1+\tau I)}$$

SPATIAL RESOLUTION = f(d)

$$\tau = \tau(R)$$

Fig. 3: **Gamma-Beam** Densitometry, A Schematic

All such transient and steady-state measurements were then compared to numerical predictions, generated with SANSMIC,[10,11] in order to assist in the qualification of this code for use in actual SPR-cavern applications.

EXPERIMENTAL RESULTS VERSUS NUMERICAL PREDICTIONS

Figure 4 shows a photograph of the traversable gamma-beam densitometer and the salt cavity pressure vessel. Figure 5 shows a salt cavity test specimen. As before'[4], salt cores were machined hollow from one end, leaving the circular wall and cavity bottom as an integral unit. Nominal pretest dimensions were: OD = 9.17 cm, ID = 5.08 cm, cavity depth = 20.32 cm, and overall sample height = 22.86 cm. Prior to leaching, each cavity was filled with saturated brine, then pressurized to 13.9 MPa. Pressure was held constant at this level for the duration of each experiment, and all experiments were conducted at a temperature of 23°C.

Table 1 gives a summary of the leaching test conditions. The primary independent variable in these experiments was the relative vertical position of the injection and withdrawal lines. All leaching experiments were conducted for essentially the same average flowrate and for the same total withdrawal time.

Present test conditions were consistent with criteria reported by Saberian[7] for the attainment of a turbulent injection plume and turbulent natural convection in the wall boundary layer. However, the physical length scale of these experiments was significantly less than actual cavern dimensions. This experimental limitation would be expected to impact comparisons with numerical predictions for those portions of the transient simulation and modelling which are length-scale dependent (e.g., modelling of the turbulent plume and mixing phenomena which occur during the injection/withdrawal period). Other models in SANSMIC are assumed to be length-scale independent (e.g., dissolution-rate and diffusion models). Hence, data obtained during the post-injection (return-to-equilibrium) pariod would be expected to provide a more valid basis for comparison. Present results tended to confirm these arguments.

Figures 6 and 7 show the results from the "direct" leaching experiment (LCH1). Here, fresh water was injected near the cavity bottom (X = 1.27 cm) while brine was withdrawn near the cavity top (X = 19.05 cm). The gamma beam was positioned at X = 6.22 cm for the transient portion of this experiment.

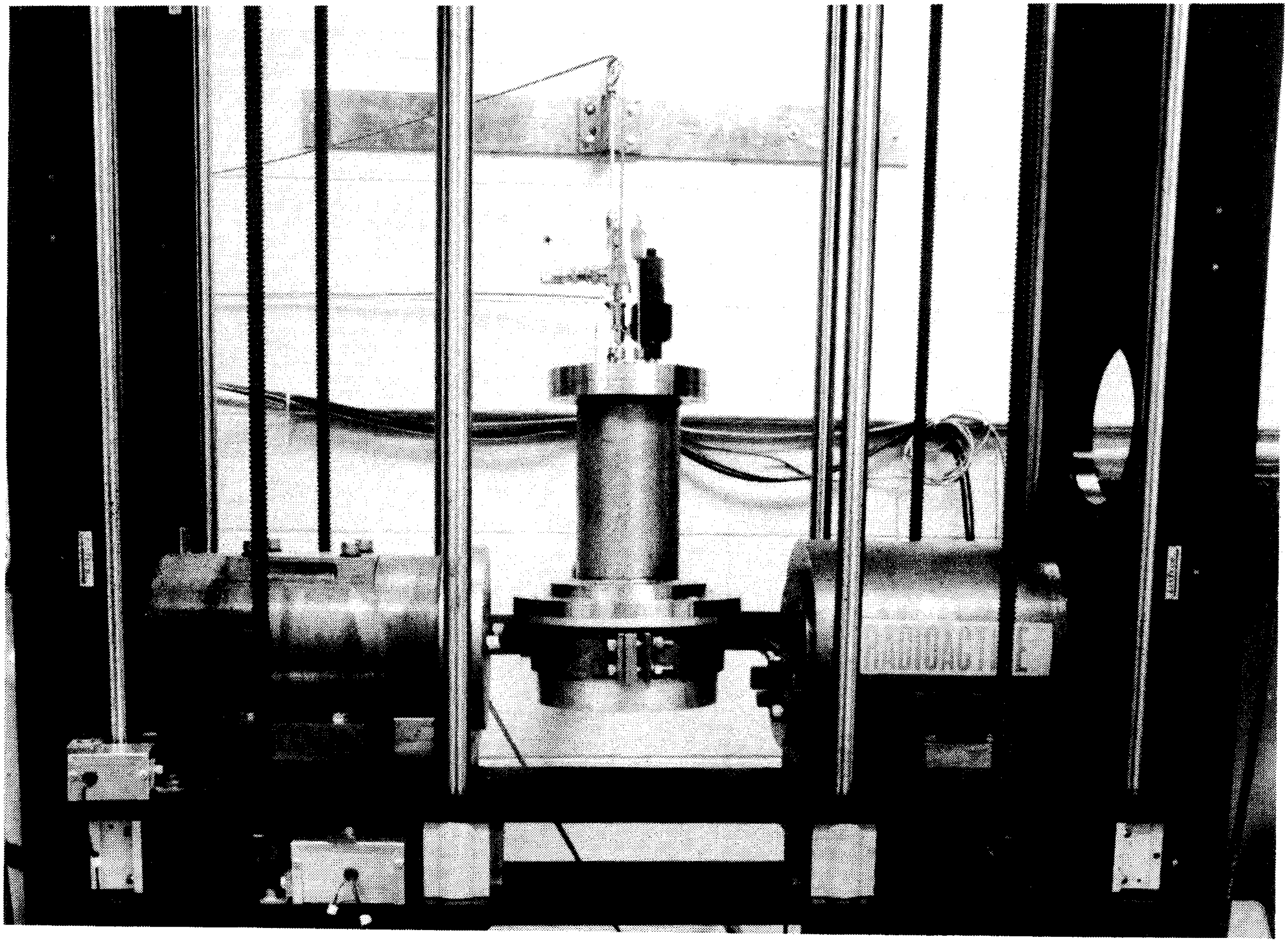

Fig. 4: Photograph of Gamma-Beam System and Test Vessel

Fig. 5: Photograph of Salt Cavity Model

SUMMARY OF TEST CONDITIONS

EXP.	X_{INJ} (IN) (cm)	X_{WD} (IN) (cm)	$\bar{Q}_{WD}$ (cc/min)	t_{WD} (min)	$\bar{\rho}_{B,WD}$ (g/cc)	$\frac{\bar{\rho}_{B,WD}-1}{\rho_{SB}-1}$
LCH1	0.50 (1.27)	7.50 (19.05)	16.33	60	1.11	**.54**
LCH2	7.50 (19.05)	0.50 (1.27)	15.78	60	**1.16**	**.79**
LCH3	2.00 **(5.08)**	4.00 (10.16)	15.47	60	1.10	**.50**

Table 1: Summary of Test Conditions

Figure 6 shows the transient results. As discussed in the previous section, R(t) yielded a quantitative measurement of the combined effects of the total salt-wall recession occurring up to time t and the brine salinity existing at time t (pathlength averaged across the cavity interior). Consequently, since these two beam-attenuation mechanisms could not be explicitly separated, the SANSMIC code was updated to allow a comparison of measured and predicted results in R versus t coordinates. The defining equations for the gamma-beam system (recall Fig. 3) were input to this code, along with measured attenuation coefficients and initial material thicknesses. Numerical predictions of sait wall recession and brine salinity at the gamma-beam location were then mathematically converted into the predicted R(t) response shown in Fig. 6.

During the injection/withdrawal period, R(t) showed an increasing trend due to continuous reductions in brine salinity and in the thickness of solid salt. Immediately following the cessation of brine withdrawal, an exponential-like decay in R(t) was observed. During this return-to-equilibrium period, beam attenuation was dominated by increases in brine salinity (occurring over a large pathlength, i.e., the cavity interior), versus the continued, but asymptotically-decreasing, salt-wall recession rate. Measured and predicted count-rate levels were seen to be in excellent agreement at the end of the post-leaching period, indicating that total salt-wall recession was accurately predicted in this case. As a result of this observation, minor differences observed during the injection/withdrawal period were most likely related to "plume effects". To expand on this issue, refer back to Fig. 1. Consider a horizontal plane through the turbulent plume region. Modelling in SANSMIC assumes a "fully-mixed" plume, and thus does not attempt to model radial variations in brine salinity. While such an assumption is justifiable on a cavern scale, such "fully-mixed" conditions most likely were not achieved in the laboratory-scale experiments. In the small-scale cavities used here, the core of the buoyant plume may have contained water of a somewhat lower salinity than the surrounding liquid. Since beam attenuation is controlled by a pathlength-averaging process, passage of the beam through a lower-salinity core region

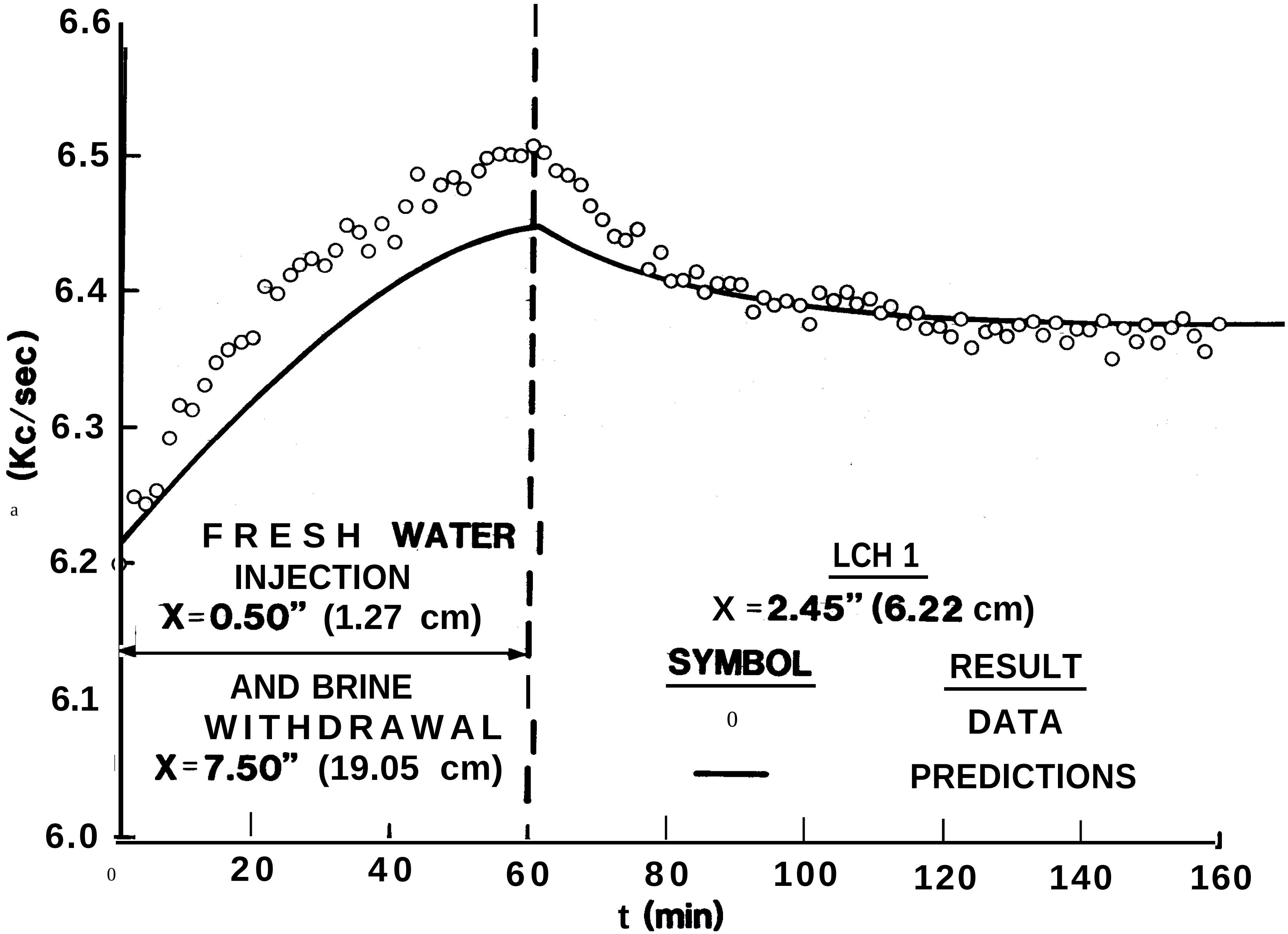

Fig. 6: Transient Count-Rate Distribution, LCH1, Data vs. Predictions

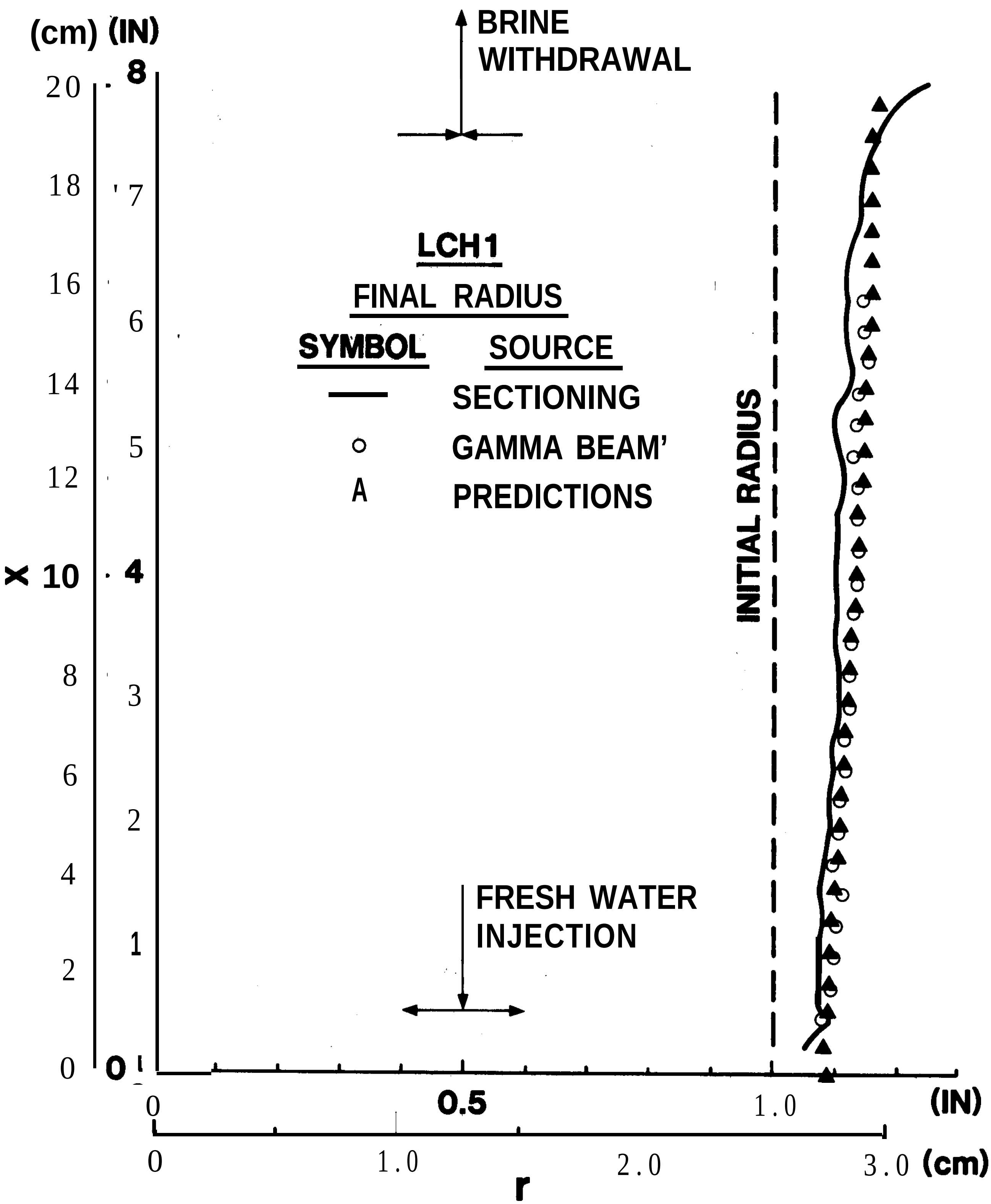

Fig. 7: Post-Test Cavity Shapes, LCH1, Data vs. Predictions

would dictate less attenuation, and thus a slightly higher count rate, than predicted by SANSMIC. Such effects were also observed during the oil-withdrawal experiments[4].

Figure 7 shows a comparison of predictions and measurements of final cavity shapes. The radial scale in this, and subsequent, cavity-shape plots has been magnified by a factor of five over the vertical scale to better illustrate the shape-change features. Injection and withdrawal locations, and the initial cavity radius, are shown for reference.

The final shape for this direct-leaching procedure was seen to remain essentially cylindrical. Some minor degree of flaring (increasing radius with increasing vertical distance) was evident. The two measurement techniques yielded essentially the same result (the sectioning results being an average of two r(X) profiles measured 180° apart, on a plane selected at random[4]). Any differences between these two measurement techniques can, therefore, be partially attributed to asymmetries in final cavity shape. The numerically-predicted shape is in very good agreement with the data, as seen in Fig. 7.

Final cavity volume was measured to be 532 cm^3 versus a predicted value of 531.1 cm^3. For an initial cavity volume of 411.9 cm^3, total salt recession (i.e., change in cavity volume) was predicted to within 0.8% of the measured result.

Figures 8 and 9 show the results from the "reverse" leaching experiment (LCH2). Here, the injection and withdrawal lines from LCH1 were “reversed”, yielding fresh-water injection at X = 19.05 cm and brine withdrawal at X = 1.27 cm. The gamma beam was positioned at X = 15.11 cm for the transient portion of this experiment.

Figure 8 shows the transient results. In this case, the liquid within the cavity tended to remain in a “stably-stratified” state, injected fresh water being continually supplied to the region near the top of the cavity, while nearly-saturated brine was withdrawn from a position in close proximity to the cavity bottom. As a result, the R(t) response did not exhibit an instantaneous positive change upon the onset of leaching, as was

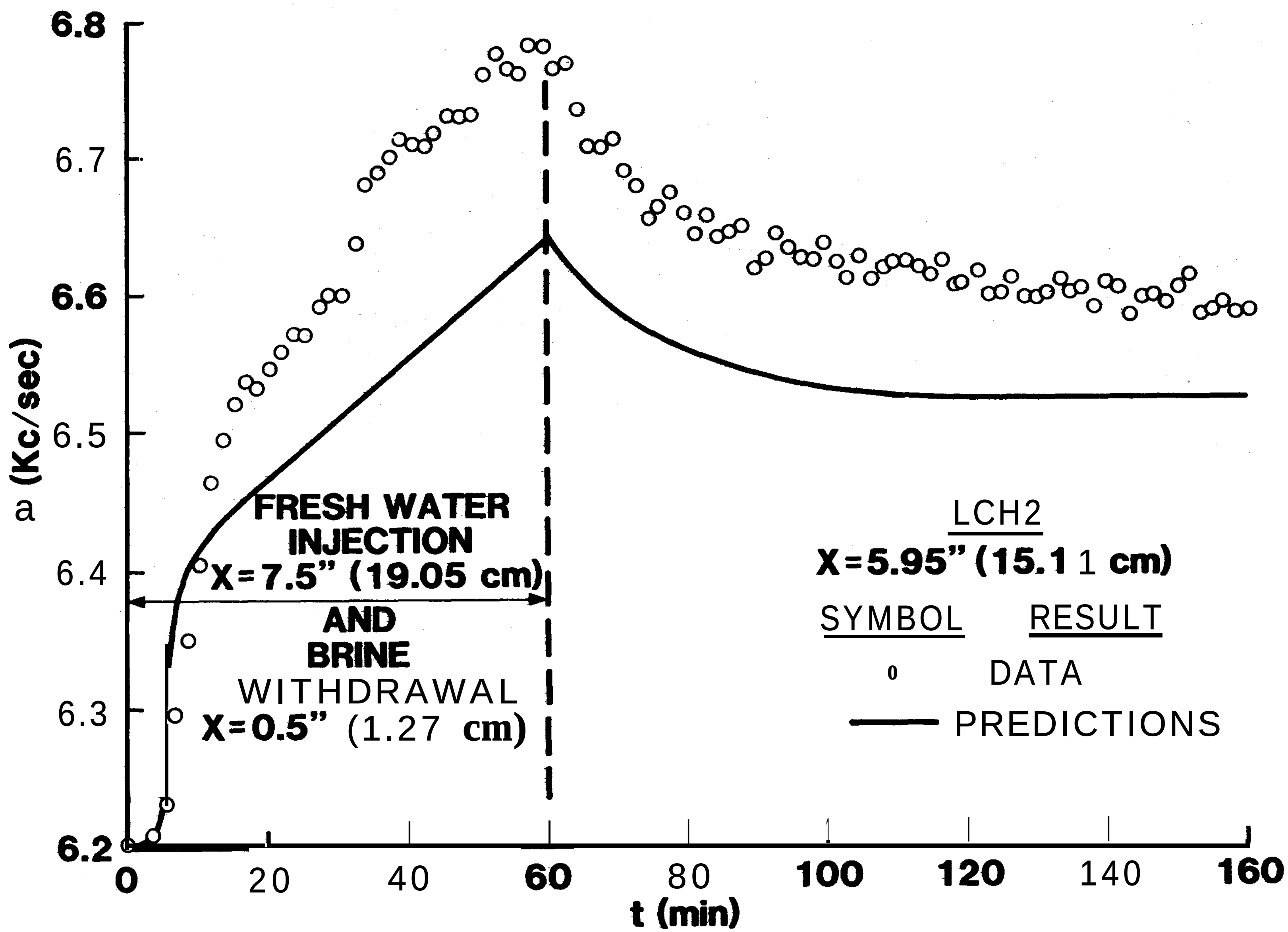

Fig. 8: Transient Count-Rate Distribution, LCH2, Data vs. Predictions

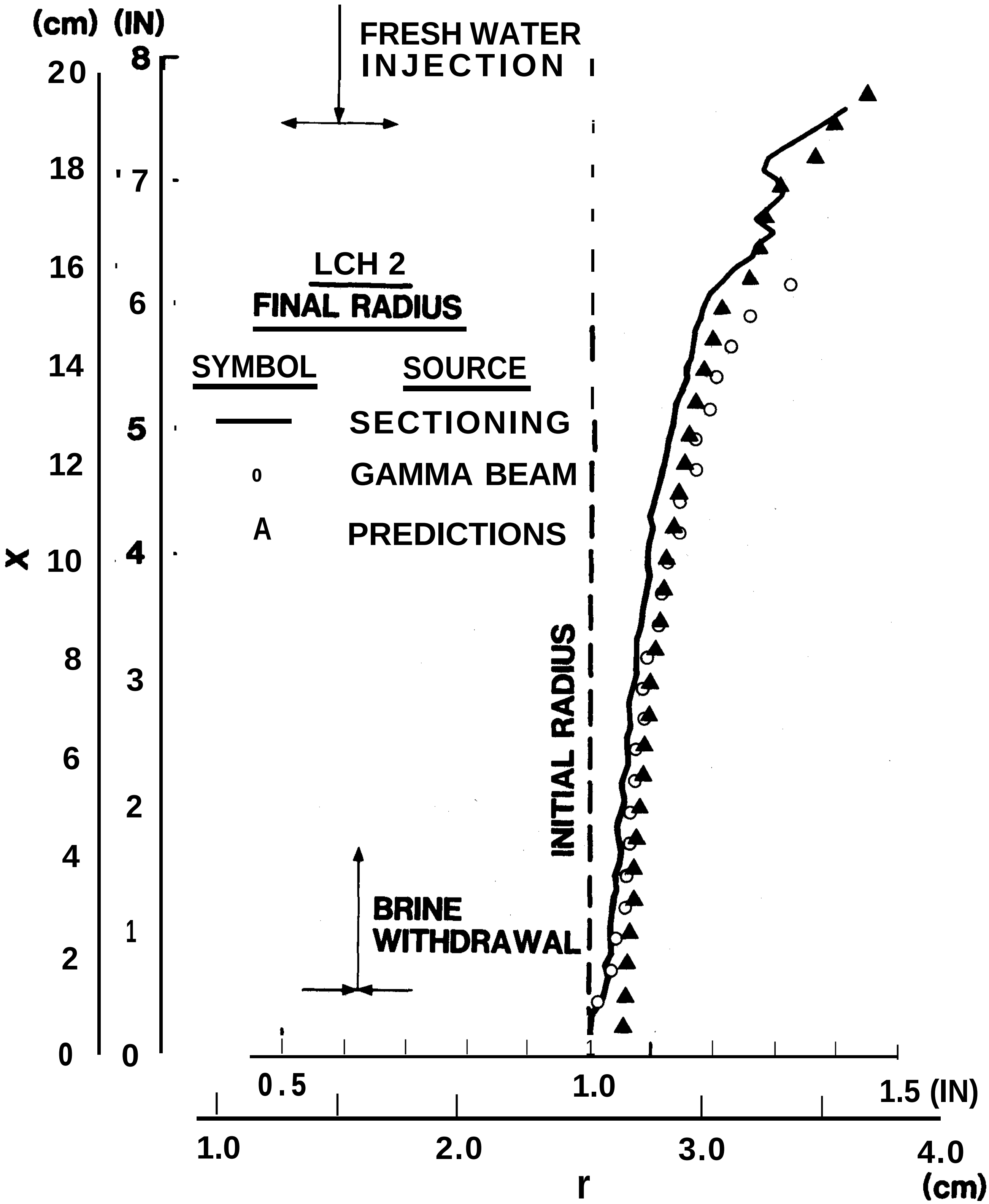

Fig. 9: Post-Test Cavity Shapes, LCH2, Data vs. Predictions

witnessed in LCH1 . Rather, a finite time period (of the order of several minutes) was required before the effects of fresh-water injection were witnessed at the gamma-beam location. The measured R(t) response was reasonably predicted during the first half of the injection/withdrawal period. However, at 35 to 40 minutes Into this active-leaching period, an abrupt increase, or "shift", occurred in the measured response, whioh essentially doubled the eount-rate difference between the measured and predicted ourves (from ≈ 100 counts/sec to ≈ 200 counts/sec). An exponential-like decay in R(t) was again found to occur during the post-withdrawal period. The "shape" of the predicted R(t) curve matched the data during this period, but the above-noted ≈ 100 count/sec difference remained at equilibrium. This difference translated into a discrepancy between predicted and measured recession of 0.13 cm, as compared to'a total predicted recession of 0.53 cm, Post-test seotioning of this specimen showed that surfaoe "pitting" had occurred in the upper regions of the cavity during leaching, i.e., a large-scale roughness pattern had formed on the surfaoe contour. Beam passage through a localized surface depression could easily account for the 0.13 cm discrepancy noted above. Overall cavity shape was well predicted, as discussed below.

Figure 9 shows a comparison of measured and predicted cavity shapes. Reverse leaching resulted in the classic “morning-glory” (or highly-flared) shape. Most of the shape change occurred in the upper regions of the cavity, near the injection location, while essentially no shape change occurred in the vicinity of the withdrawal location. These observations are consistent with the presence of a stably-stratified liquid during the leaching process. As can be seen in Fig. 9, the two measurement techniques yielded closely matching profiles in the bottom half of the cavity, but showed some departure in the upper regions.

Once again, the numerically-predicted shape showed good agreement with the data. The primary feature of this shape, the large flare at the top of the cavity, was well predicted, A minor amount of shape change was predicted to occur below the withdrawal elevation, whereas the data showed no measureable shape change in this region.

Final cavity volume for this case was measured to be 560 cm^3 versus a predicted final volume of 562.7 cm^3. Total change in cavity volume was thus predicted to an accuracy of 1.8%.

The final experiment conducted during this study represented a variation of the direct-leaching procedure. In this case, referred to as "localized-direct" leaching, injection was below withdrawal, but the two locations were in proximity to one another (a vertical separation distance equal to one-quarter of the total cavity depth). Injection occurred at X = 5.08 cm and withdrawal at X = 10.16 cm. The gamma beam was positioned at X = 7.49 cm for the transient measurements. Results are shown in Figs. 10 and 11.

Figure 10 shows the transient results. Agreement between the numerical predictions and the measurements is seen to be quite good. Transient plume effects are again thought to be the cause of those differences which evolved during the active-leaching period (recall discussions concerning Fig. 6).

Figure 11 shows a comparison of the predicted and measured final cavity shapes. Both the gamma-beam and the sectioning measurements show shape change to originate immediately below the injection location, i.e., a "step change" in cavity radius formed at this elevation. "Localized" leaching is seen to occur above this step, between the injection and withdrawal elevations, resulting in an essentially constant-radius region. The modest flare which evolved in the upper extent of the cavity indicates that some fraction of the injected fresh water bypassed the withdrawal line, buoyantly rose towards the top of the cavity, and preferentially leached the salt in this region.

The numerically-predicted shape possesses these same basic features. Recession is reasonably predicted over most of the cavity surface area, the only notable discrepancies occurring at the extreme lower and upper elevations. A predicted step change in cavity radius is seen to form, but at a location somewhat below the experimentally-defined elevation. The extent of flare formation at the top of the cavity is underpredicted.

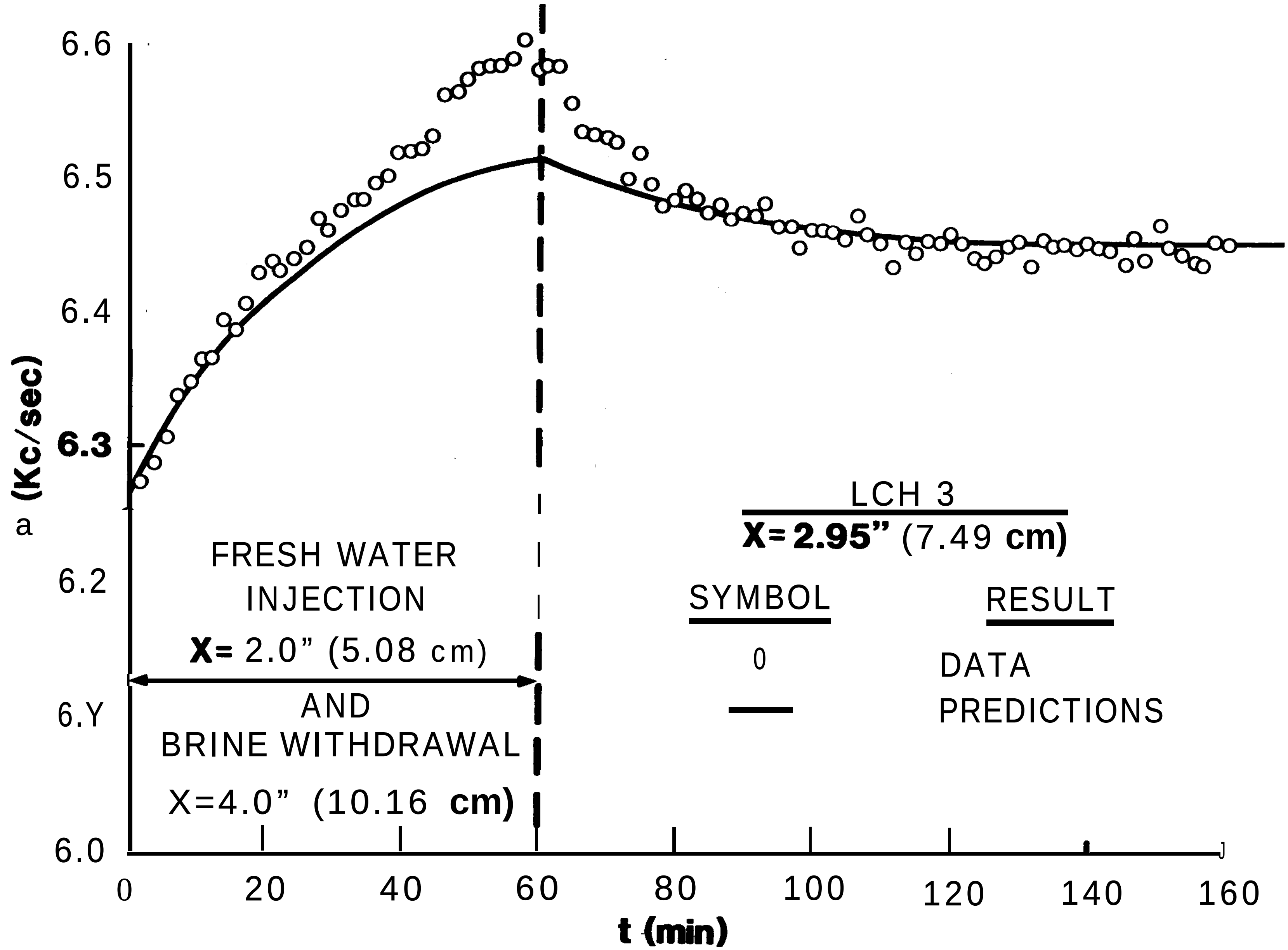

Fig. 10: Transient Count-Rate Distribution, LCH3, Data vs. Predictions

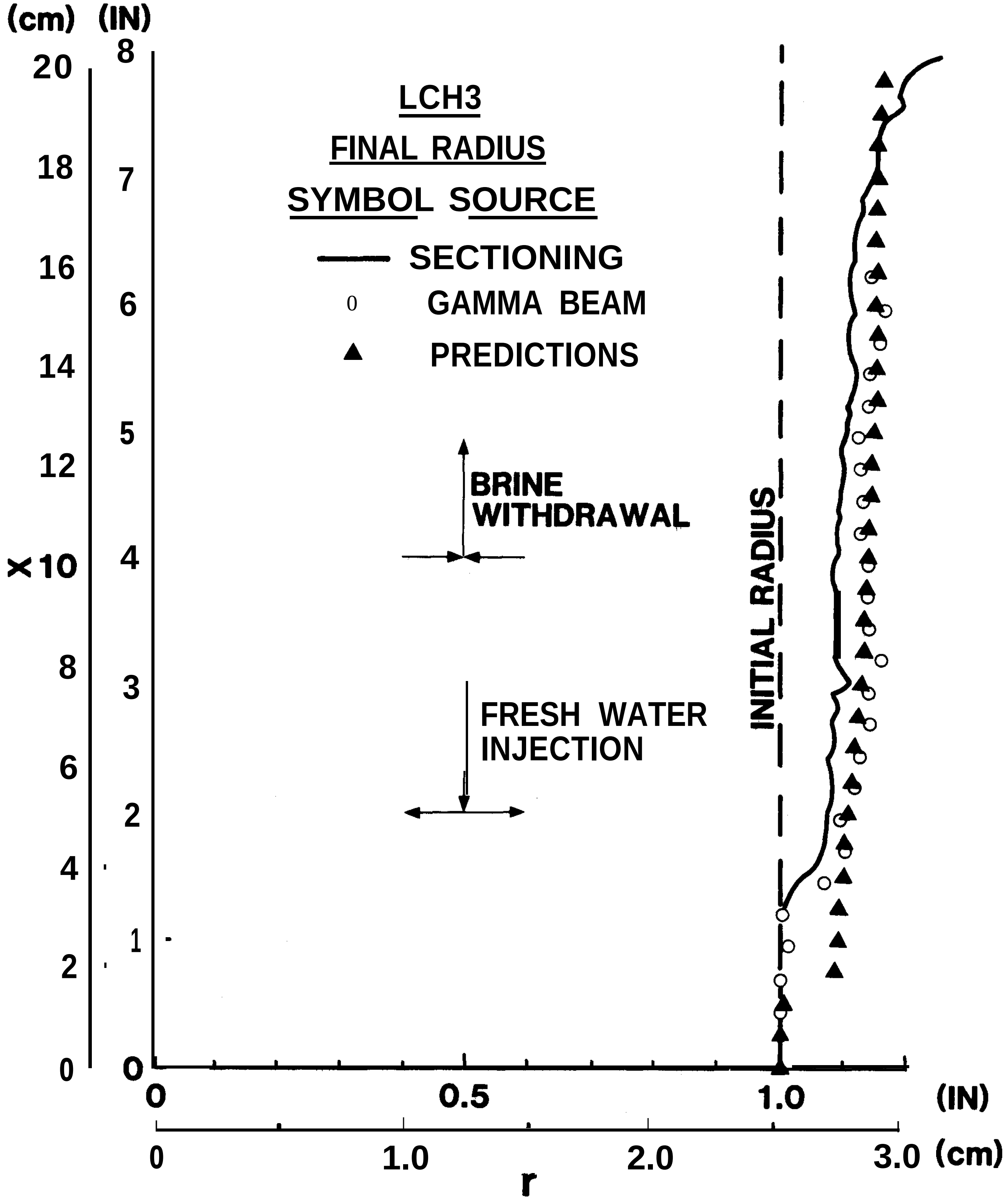

Fig. 11: Post-Test Cavity Shapes, LCH3, Data vs. Predictions

In this case, the measured final cavity volume was 520 cm^3 compared to a predicted value of 529.5 cm^3. Total volumetric change was thus predicted to within 8.8% of the measured value.

Summarizing the modelling of these three experiments, both transient and steady-state results were well predicted. For direct and reverse leaching (the two most-utilized methods), cavity volumetric change was predicted by SANSMIC to 1-2% accuracy. For the more complex, localized-direct leaching, volumetric change was predicted to $\approx$ 9%. Additional comparisons are under way between predicted and measured cavern shapes (generated during actual field operations) in order to further validate the SANSMIC code.

CONCLUSIONS

Based on experimental results for salt-cavity leaching, and on comparisons of these results with numerical predictions, the following observations were made:

1. The relative vertical position of the fresh-water-injection and brine-withdrawal lines can have a significant effect on salt cavity shape change.

2. Gamma-beam densitometry can be used as a non-intrusive diagnostic technique to characterize transient phenomena which occur during leaching, as well as to measure resultant post-test cavity shapes.

3. Numerical predictions generated with the Sandia Solution-Mining Code[10,11] were found to be in good agreement with both transient and steady-state results measured during this investigation.

REFERENCES

1. Durie, R. W. and Jessen, F. W., "Mechanism of the Dissolution of Salt in the Formation of Underground Salt Cavities," Soc. Petroleum Engineers Journal, June, 1964, pp. 183-190.
2. Durie, R. W. and Jessen, F. W., "The Influence of Surface Features in the Salt Dissolution Process," Soc. Petroleum Engineers Journal, September, 1964, pp. 275-281.
3. Kazemi, H. and Jessen, F. W., "Mechanism of Flow and Controlled Dissolution of Salt in Solution Mining," Soc. Petroleum Engineers Journal, December, 1964, pp. 317-328.
4. Jessen, F. W., "Total Solution Mechanism," AIME Transactions, Vol. 250, December, 1971, pp. 298-303.
5. Von Schonfeldt, H., "Model Studies in Solution Mining," Proc. 4th International Symposium on Salt, N. Ohio Geologic Society, Houston,TX, 1973.
6. Chang, C., Vliet, G. C. and Saberian, A., "Natural Convection Mass Transfer at Salt-Brine Interfaces," Journal of Heat Transfer, Vol. 99, November 1977, pp. 603-608.
7. Saberian, A. and Podio, A. L., "A Computer Model for Describing the Development of Solution-Mined Cavities," IN SITU, 1(1), 1977, pp. 1-36.
8. Pottier, M. and Esteve, B., "Simulation of Gas Storage Cavity Creation by Numerical Methods," Proc. 4th International Symposium on Salt, N. Ohio Geologic Society, Houston, TX, 1973.
9. Nolen, J. S., et al, "Numerical Simulation of the Solution Mining Process," Soc. of Petroleum Engineers, SPE-4850, European Spring Meeting, Amsterdam, The Netherlands, May, 1974.
10. Russo, A. J., "A Solution Mining Code for Studying Axisymmetric Salt Cavern Formation," Sandia National Laboratories Technical Report, SAND81-1231, September 1981.

11. Russo, A. J., "A User's Manual for the Salt Solution Mining Code, SANSMIC," Sandia National Laboratories Technical Report, SAND83-1150, September 1983.

12. Morton, B. R., Taylor, G., and Turner, J. S., "Turbulent Gravitational Convection from Maintained and Instantaneous Sources," Proc. Royal Society, Series A, Vol. 234, No. 1196, January 1956, pp. l-23.

13. Turner, J. S., "Buoyancy Effects in Fluids," Cambridge University Press, New York, NY, 1973.

14. Reda, D. C. and Russo, A. J., "Experimental Studies of Oil Withdrawal from Salt Cavities via Fresh-Water Injection," Sandia National Laboratories Technical Report, SAND83-0347, March 1984.

15. Reda, D. C., Hadley, G. R. and Turner, J. R., "Application of the Gamma-Beam Attenuation Technique to the Measurement of Liquid Saturation for Two-Phase Flows in Porous Media," Proc. of the 27th International Instrumentation Symposium, Instrument Society of America, Indianapolis, IN, April 1981, pp. 553-568.

Distribution:

E. E. Chapple, PMO-681 (6)
U. S. DOE SPRPMO
900 Commerce Road East
New Orleans, LA 70123

L. Rousseau
U. S. DOE SPRPMO
900 Commerce Road East
New Orleans, LA 70123

V. Kilroy
U. S. DOE SPRPMO
900 Commerce Road East
New Orleans, LA 70123

Larry Pettis
U. S. Department of Energy
Strategic Petroleum Reserve
1000 Independence Avenue, SW
Washington, DC 20585

Bill Wilson
U. S. Department of Energy
Strategic Petroleum Reserve
1000 Independence Avenue, SW
Washington, DC 20585

Aerospace Corporation (2)
800 Commerce Road East, Suite 300
New Orleans, LA 70123
Attn: E. Katz
R. Merkle

Jacobs/D'Appolonia Engineers (2)
P. 0. Box 23308
Harahan, LA 70183
Attn: P. Campbell
H. Kubicek

POSSI (2)
850 S. Clearview Pkwy.
New Orleans, LA 70123
Attn: Dub Butler
K. E. Mills

W. Marquardt
Parsons-Gilbane
800 Commerce Road West
New Orleans, LA 70123

Alfred H. Medley
Fenix & Scisson, Inc.
1401 South Boulder
Tulsa, OK 74119

Dr. Alfred Finkenwirth
LANZSTR.25
6200 Wiesbaden
West Germany

Gayle D. Petrick, P.E.
Diamond Crystal Salt Company
St. Clair, MI 48079

Eng. Diamantino Mendonca
Socio-Gerente
Sondagens E. Fundacoes A. Cavaco, LDA.
Av. Eng. Durate Pacheco, 21-2.°
1000 Lisbon
Portugal

Ir. Th. H. Wassmann
Manager, Minerals Department
Akzo Zout Chemie Nederland bv
Boortorenweg 20
7554 RS Hengelo (O)
The Netherlands

Jerome S. Blank
Kalium Chemicals
Suite 1120
600 South Cherry Street
Denver, CO 80222

Joseph Didier Martinez, CPGS, PE
P. O. Drawer J.D.
University Station
Baton Rouge, LA 70893

Elmar L. Goldsmith
Kalium Chemicals
400 Bank of Canada Building
Regina, Saskatchewan S4P OM9
Canada

Hans Y. Tammemagi, PhD
RE/SPEC Ltd.
4616 Valiant Drive, NW - Suite 201
Calgary, Alberta T3A OX9
Canada

Hans-J. Doering
Ruhrgas Aktiengeaellschaft
Referent Technische Planung - Lagerstatten
Huttropstrasse 60
D-4300 Essen 1
West Germany

Dr. Adrian J. Van Der Hoeven
Nord-West Kavernengesellschaft
MIT Beschrankter Haftung
2940 Wilhelmshaven 31
Kavernenfeld K-6
West Germany

James H. Huizingh
Texasgulf Chemicals Co.
P. 0. Box 1208
Moab, UT 84532

E. Leon Cook
PPG Industries, Inc.
P. 0. Box 1000
Lake Charles, LA 70602

Diamond Shamrock Corp.
P. 0. Box 1000
Pasadena, TX 77501
Attn: R. G. LaFortune

A. Saberian and Associates
3305 Northland Drive #407
Austin, TX 78731

Solution Mining Research Center (50)
812 Muriel St.
Woodstock, IL 60098
Attn: H. W. Fiedelman

PB-KBB, Inc. (2)
11999 Katy Freeway, #600
P. 0. Box 1967.2
Houston, TX 77024
Attn: W. M. Bishop
R. W. Blair

1510 J. W. Nunziata
1511 G. G. Weigand
1512 J. C. Cummings
1512 D. C. Reda (25)
1512 A. J. Russo
1513 D. W. Larson
1513 R. J. Gross
1520 D. J. McCloskey
1530 L. W. Davison
1540 W. C. Luth
6257 J. K. Linn (6)
3141 C. M. Ostrander (5)
3151 W. L. Garner (3)
for DOE/TIC (Unlimited Release)
3154-3 C. H. Dalin (25)
DOE/TIC
8424 M. A. Pound